Pis'ma v ZhETF, vol. 103, iss. 5, pp. 365 – 371 © 2016 March 10

Effect of magnetic field on the intermediate phase in $Mn_{1-x}Fe_xSi$: spin-liquid vs. fluctuations scenario

S. V. Demishev[a,b1)], I. I. Lobanova[a,b], A. V. Bogach[a], V. V. Glushkov[a,b], V. Yu. Ivanov[a], T. V. Ischenko[a], N. A. Samarin[a], N. E. Sluchanko[a], S. Gabani[c], E. Čižmár[d], K. Flachbart[c], N. M. Chubova[e], V. A. Dyadkin[e,f], S. V. Grigoriev[e]

[a] Prokhorov General Physics Institute of RAS, 119991 Moscow, Russia

[b] Moscow Institute of Physics and Technology, 141700 Dolgoprudny, Russia

[c] Institute of Experimental Physics SAS, 040 01 Košice, Slovak Republic

[d] P.J. Šafárik Univesity in Košice, SK-04001 Košice, Slovak Republic

[e] Petersburg Nuclear Physics Institute, 188300 Gatchina, Russia

[f] Swiss-Norwegian Beamlines at the European Synchrotron Radiation Facility, 38000 Grenoble, France

Submitted 1 December 2015
Resubmitted 18 January 2016

We report results of the magnetic field influence on the chiral spin liquid state in $Mn_{1-x}Fe_xSi$ single crystal with iron content $x = 0.108$ in proximity of a hidden quantum critical point. The use of small angle neutron scattering data together with magnetic susceptibility measurements down to 0.4 K and precise magnetoresistance measurements in the temperature range 2–20 K in magnetic field up to 5 T allowed us to construct the magnetic phase diagram of this compound in which at low magnetic fields $B < 0.15$ T an intermediate phase with short-range magnetic order exists in a wide temperature range $0.62 < T < 9.1$ K. It was found that the increase of magnetic field first results in a suppression of transition into spiral phase with long-range magnetic order at very low temperatures, and then induces a transition of the intermediate phase into a spin-polarized (ferromagnetic) phase with lowering temperature. The temperature of this transition T_{SP} increases with magnetic field logarithmically, $T_{SP} \sim \log(B)$, and results in formation of a singular point on the magnetic phase diagram located at $T \sim 8.5$ K and $B \sim 3.5$ T, which may be either a triple or a critical point. The possible spin-liquid nature of the intermediate phase is discussed.

DOI: 10.7868/S0370274X16050076

1. Spiral magnets $Mn_{1-x}Fe_xSi$ are characterized by presence of unusual magnetic phases, which are intermediate between common paramagnetic phase (PM) and spiral magnet (SM) phase with long-range magnetic order [1–4]. These intermediate phases (IP) may be detected either on $B - T$ [1, 3] or on $T - x$ [1, 2, 4] magnetic phase diagrams. Several theoretical studies also predict phases with intermediate magnetic order for MnSi based solids [5, 6]. These results may be qualitatively understood following experimentally supported similarity between spiral magnets and cholesteric liquid crystals [7], in which the considered intermediate phases appear as a magnetic analog of the blue fog phases [5, 7, 8]. The IP are also referred as spin liquid (or chiral spin liquid) states due to straightforward analogy from general physics, where the paramagnetic phase, spiral phase with long-range order (LRO) and intermediate phase may be considered as magnetic replicas of the common gas, solid and liquid phases [5]. Nevertheless, sometimes the aforementioned description of the intermediate magnetic phases is disputed, and these specific states are treated as regions of pronounced magnetic fluctuations in the phase diagram [9]. In any case these specific phases are of magnetic nature and thus may be affected by external magnetic field; however the influence of magnetic field on the phases with intermediate magnetic order has not been studied systematically so far. At the same time an analogy with liquid crystals suggests that the external field may noticeably change the corresponding phase diagram [8].

In the present Letter, we aim to study experimentally the influence of magnetic field on the intermediate magnetic phase in $Mn_{1-x}Fe_xSi$ developing in proximity to the hidden quantum critical point at $x^* \sim 0.11$

1) e-mail: demis@lt.gpi.ru

[4]. For this iron concentration the transition into SM phase with long-range magnetic order is expected to be suppressed and an intermediate magnetic phase may be observed at temperatures below $T_s \sim 9{-}10$ K in zero magnetic field, so that the quantum phase transition corresponding to a loss of long-range magnetic order becomes hidden inside the IP [4]. Therefore the choice of the sample with this iron concentration has an advantage because the region of existence of the intermediate phase is much extended with respect to pure MnSi [2]. Based on magnetic susceptibility study down to very low temperatures, polarized neutron scattering experiments and precise magnetoresistance measurements we will show that this intermediate phase may be strongly affected by magnetic field resulting in a specific shape of the $B{-}T$ phase diagram with a singular point. In conclusion, possible arguments that the IP in studied case is a kind of spin liquid phase rather than a region of fluctuations will be provided.

2. The single crystal of $Mn_{1-x}Fe_xSi$ with determined by Electron Probe Micro-Analysis (EPMA) iron concentration $x = 0.108$ was synthesized by both Czochralski and Bridgman methods. Assuming the composition formula $(Mn_{1-x}Fe_x)_{1+y}Si_{1-y}$ we found that the crystal stoichiometry was about $y \sim 0.01$, comparable with the absolute error of our EPMA measurements. The quality of the sample was controlled by X-ray Laue diffraction. The magnetization and magnetic susceptibility data in magnetic field up to 5 T were obtained with the help of SQUID magnetometer (Quantum Design) equipped with a He^3 insert, which allowed to extend susceptibility measurements down to 0.4 K. The resistivity data $\rho(T)$ were measured by standard DC four probe technique at temperatures 1.8–300 K with the help of special installation (Cryotel Ltd.) characterized by relative accuracy of resistivity measurements $\sim 10^{-5}$ in fixed magnetic field up to 5 T together with the temperature stabilization/measurement precision level of about 1 mK for temperatures below 60 K. The details concerning polarized small angle neutron scattering (SANS) technique and the corresponding data analysis procedure may be found elsewhere [2].

The study of the magnetic phase diagram performed in present work was based on a combination of two methods. The first method consists of a comparative study of the temperature dependence of magnetic susceptibility $\chi(T)$ and related evolution of the neutron scattering data [2]. It was established, that extrema of the derivative $\partial\chi/\partial T$ clearly mark the *qualitative* change of neutron diffraction pattern, which allows to identify various magnetic phases including PM, SP, and IP, and determine the characteristic transition temperatures [2]. Namely, the minimum of the $\partial\chi/\partial T$ temperature dependence at T_s corresponds to transition from the paramagnetic phase into the intermediate phase, whereas the maximum denotes the onset of long-range magnetic order in the spiral magnet phase [2]. It is worth nothing, that in Ref. [2] the temperature T_s of the transition into IP, which is well defined experimentally, were treated as a "crossover" temperature despite the fact of the qualitative change of the SANS map just at T_s favors the explanation based on real magnetic transition in agreement with the liquid-crystal analogy [5, 8, 7].

However, the magnetic susceptibility analysis is limited to the range of low magnetic fields. In high magnetic fields the susceptibility and magnetization characteristic features namely become too broad and, as it was shown in [10], susceptibility data and extrema of its derivative do not provide correct information about phase boundaries. It may be shown that, in order to establish the location of phase transitions on the $B{-}T$ magnetic phase diagram in high magnetic fields, it is instructive to analyze the magnetoresistance data [10]. The latter observation is explained by the fact that in $Mn_{1-x}Fe_xSi$ magnetic scattering dominates and all other possible contributions to magnetoresistance (including Drude-type magnetoresistance [10]) are negligible [10, 11]. In addition, in the paramagnetic phase of $Mn_{1-x}Fe_xSi$ the negative magnetoresistance follows the universal scaling $\Delta\rho/\rho = -aM^2(B,T)$ [10, 11]; hereafter $M(B,T)$ denotes the sample magnetization and a stands for the proportionality coefficient depending on iron concentration. The deviations of scaling behavior may serve as marks for transitions from the PM phase into magnetically ordered phases [10]. For example, the maximum on the temperature dependence of the absolute value of magnetoresistance in fixed magnetic field $|\Delta\rho/\rho(B = \text{const}, T)|$ corresponds to a transition between the paramagnetic phase and the spin-polarized (field induced ferromagnetic) phase [10].

Although magnetic properties of MnSi based solids are often interpreted in terms of itinerant models [12] the LDA calculations suggest localization of the spin density on Mn sites [13]. Additionally, the detailed quantitative analysis of electron spin resonance in $Mn_{1-x}Fe_xSi$ [10, 11, 14] also favors the existence of localized magnetic moments (LMM) rather than the spin density distributed in the unit cell. Within the framework of the Heisenberg type LMM model the aforementioned features of high field magnetoresistance may be quantitatively understood as a consequence of Yosida scattering mechanism [15, 10]. Indeed, in the considered approach there are two scattering channels corresponding to different spin projections of the band electron,

which interaction with LMM may be accounted in the $s-d$ exchange model [15]. In the paramagnetic phase the Yosida scattering results into $\Delta\rho/\rho \sim -M^2(B,T)$ dependence [15]. The entering into a magnetically ordered state leads to redistribution of the scattering probability between different spin channels and formation of peculiarities on temperature and field dependences of magnetoresistance. For example, in the spin-polarized (SP) phase both localized and moving spins are polarized at low temperatures. For that reason the basic assumption made in [15] for two spin dependent scattering channels fails and magnetoresistance should not depend on the spin states. As a result the universal magnetoresistance scaling will be no longer valid, and any temperature dependence of the spin dependent contribution to magnetoresistance in the ferromagnetic phase will be caused by thermal fluctuations destroying the "ideally" polarized state and consequently $\Delta\rho/\rho \to 0$ for $T \to 0$. As long as the PM phase the magnetoresistance $|\Delta\rho/\rho(B = \text{const}, T)|$ grows with lowering temperature because $M(B = \text{const}, T)$ increases, it reaches a maximal absolute value just at the transition between the paramagnetic and spin-polarized phases and then drops in the spinpolarized phase [10]. In this way the considered features of magnetoresistance receive theoretical support and the analysis of magnetoresistance becomes applicable for establishing the magnetic phase diagram in the high magnetic field region.

3. To start, we will consider results obtained by the first method of determination of the magnetic phase diagram. Temperature dependences of magnetic susceptibility $\chi(T)$ and its derivative $\partial\chi/\partial T$ for magnetic fields 200–1500 Oe in the temperature range $0.4 < T < 20$ K are presented in the upper panel of Fig. 1. In the diapason $T > 2$ K $\chi(T)$ data does not depend on magnetic field and position of $\partial\chi/\partial T$ minimum $T_s = 9.1$ K remains unchanged. The Curie–Weiss approximation $\chi(T) \sim 1/(T - \Theta)$ of experimental data is valid for relatively high temperatures $T > 12$ K with the paramagnetic temperature $\Theta \sim 6.1$ K.

In contrast, the low temperature part ($T < 2$ K) may be modified substantially. For $B = 200$ Oe there is a maximum of the magnetic susceptibility derivative located at $T = 0.62$ K, which, according to Ref. [2], should mark the transition into the spiral magnet phase. However, for $B \geqslant 500$ Oe this feature is not observed. Simultaneously the section of the $\partial\chi/\partial T$ growth ($T < 2$ K) shifts to lower temperatures with magnetic field (Fig. 1, upper panel). Therefore we suppose that increase of magnetic field may result into a shift of the $\partial\chi/\partial T$ maximum to lower temperatures, so that this feature cannot be found in the temperature range available in the present study.

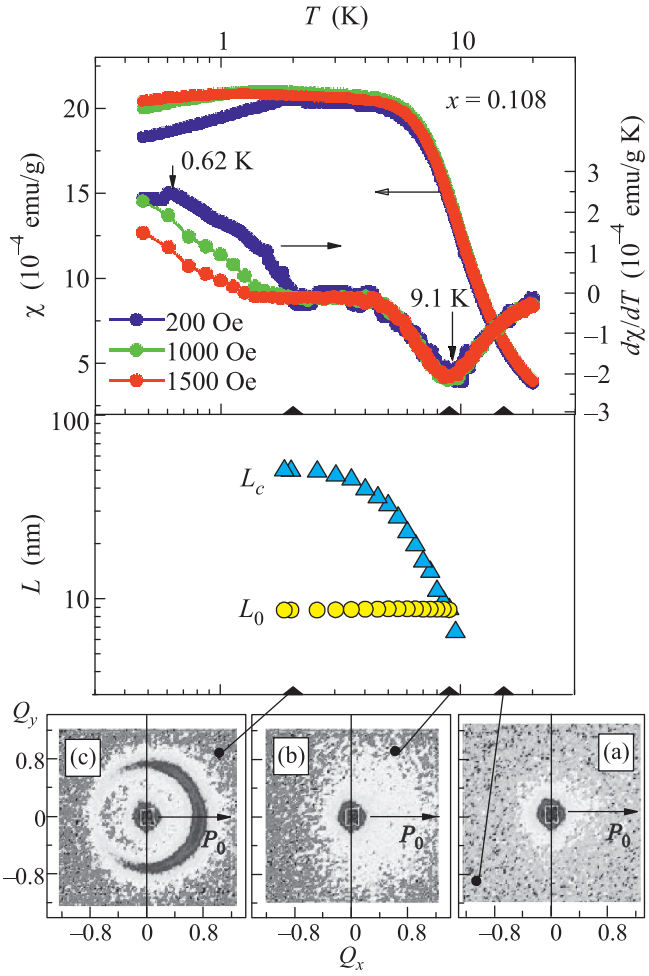

Fig. 1. (Color online) Magnetic susceptibility χ and its derivative $\partial\chi/\partial T$ as a function of temperature at various magnetic fields (upper panel). Lower panel represents temperature dependence of the helix period L_0 and coherence length L_c in the intermediate phase. Black triangles at the temperature axis denote points, where corresponding SANS maps were obtained. In SANS maps $\mathbf{P}_0$ is the vector of neutron polarization, the scale for scattering vector projections Q_x and Q_y is inversed nanometers

The temperature evolution of polarized SANS data were traced down to $T = 1.8$ K. It is visible from Fig. 1 that for temperatures above T_s the scattering pattern shows a weak diffuse scattering, which is typical for a PM phase (SANS map a). When the temperature becomes somewhat lower than T_s, the SANS map undergoes qualitative change and acquires a characteristic half-moon shape located in the direction of the neutrons polarization vector $\mathbf{P}_0$ (SANS map b). This type of diffraction picture corresponds to IP with spiral short-range order (SRO) [2]. Further decrease of tempera-

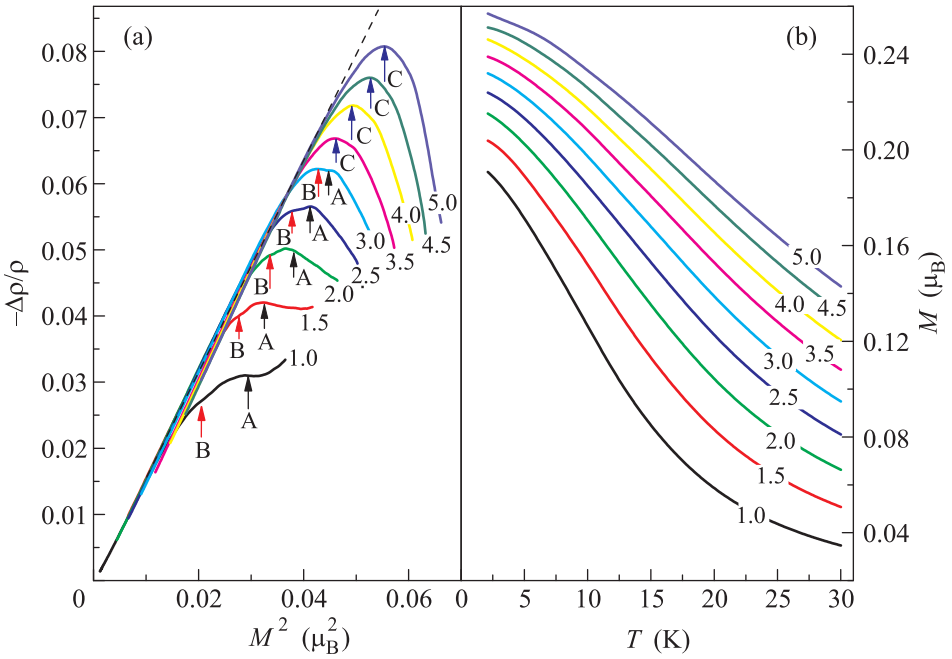

Fig. 2. (Color online) Yosida scaling of magnetoresistance (a) and magnetization at fixed magnetic fields (b). Digits near each curve correspond to magnetic fields in Tesla. The peculiarities on magnetoresistance curves (A, B, C) are the same as the magnetoresistance minima in Fig. 3. The magnetization is given in Bohr magneton per Mn ion

ture makes the half-moon structure more pronounced (SANS map c) but no distinct Bragg peaks develop up to the lowest temperature studied. Therefore, it is possible to conclude from the data of Fig. 1 that in the studied $Mn_{1-x}Fe_xSi$ sample the IP of spiral nature in low magnetic field should exist in a wide temperature range $0.62 < T < 9.1$ K and the slight increase of magnetic field may expand the range of the intermediate phase stability. This observation confirms the previous conclusion [4] concerning the proximity of studied sample to the hidden quantum critical point. It can be also noted that the observed evolution of magnetic structure is qualitatively the same as in liquid crystals which undergo transitions from the isotropic phase into phases with partial order [8].

Following the data analysis technique of SANS diffraction patterns described in [2], it is possible to find temperature dependences of the helix pitch L_0 and the coherence length of the magnetic fluctuations in the intermediate phase L_c (lower panel in Fig. 1). The latter parameter may be also interpreted as the size of coherent region of magnetic scattering. It is visible (Fig. 1) that the period of the spin spiral is almost temperature independent and for the studied sample it is about $L_0 \sim 9$ nm, which is the half of the period for pure MnSi. On the contrary, the coherence length first demonstrates a pronounced increase with lowering temperature and then saturates on the level $L_c \sim 50$ nm for $T < 2$ K.

4. For implementation of the second method it is essential to analyze magnetoresistance data in coordinates $\Delta\rho/\rho = f(M^2)$. The result is presented in Fig. 2a for different temperature dependences of magnetoresistance in fixed magnetic fields. As expected, there is a section of universal $\Delta\rho/\rho = -aM^2(B,T)$ behavior which holds in the paramagnetic phase. Temperature lowering results in an increase of magnetization (Fig. 2b) and induces departures from the Yosida-type scaling due to transitions into magnetically ordered phases (Fig. 2a). It is worth noting that the maximum of the negative magnetoresistance absolute value not only becomes more pronounced in higher magnetic field but also demonstrates some structure for $B < 3.5$ T. At the same time the corresponding features are not visible on $M(B = \text{const}, T)$ curves (Fig. 2b) that agrees with results reported previously [10].

The analysis of the ratio $\rho(B,T)/\rho(0,T)$ suggests that in the studied sample there is a superposition of two magnetoresistance minima (see Fig. 3 main panel and inset) for $B < 3.5$ T, which are denoted in Figs. 2 and 3 as A and B. It is visible that the position of the minimum B weakly depends on temperature. At the same time the minimum A shifts noticeably to higher temperatures when the magnetic field is increased up to $B \sim 3.5$ T (Fig. 3). In higher magnetic field $B > 3.5$ T no separate minima can be resolved and experimental data demonstrate the presence of the single magnetore-

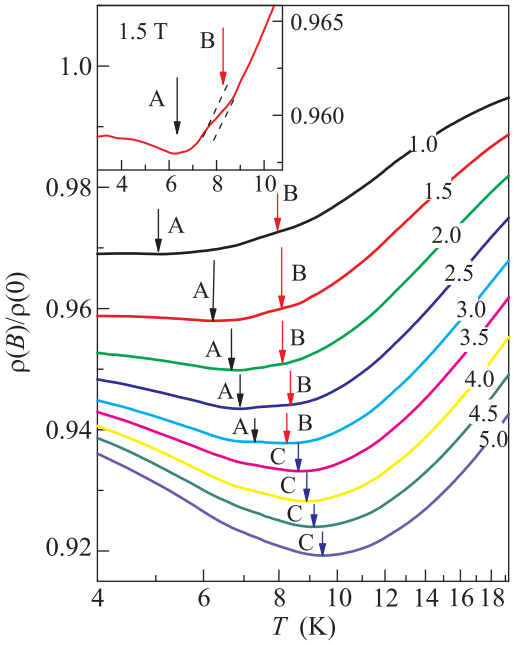

Fig. 3. (Color online) Temperature dependences of magnetoresistance in fixed magnetic fields. Digits near each curve correspond to magnetic fields in Tesla. The characteristic minima on magnetoresistance curves (A, B, C) are the same as the peculiarities in Fig. 2

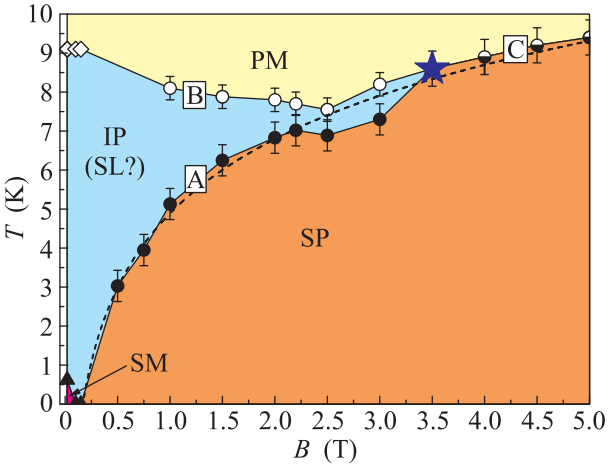

Fig. 4. (Color online) Magnetic phase diagram for the studied $Mn_{1-x}Fe_xSi$ sample with $x = 0.108$. The star denotes the position of the singular point (see text for details). Letter abbreviations corresponds to paramagnetic (PM), possible spin-liquid (SL), spin polarized (SP), and spiral magnet (SM) phase. IP stands for the intermediate magnetic phase. Phase boundaries obtained from positions of magnetoresistance minima A, B, C in Fig. 3 are denoted by the corresponding letters. Dashed line represents the logarithmic approximation of the transition into SP phase. Black triangle at $B = 0$ denotes expected transition into SM phase. The area of the SM phase is drawn according to hypothesis formulated in the text

sistance minimum C (Figs. 2 and 3). It is essential that the minima A and C in magnetoresistance data posses a strong magnitude and the minimum B exhibits only a relatively shallow feature (inset in Fig. 3). We wish to note that, although the observed anomalies are broad, they may correspond to sharp magnetic transitions [10], as long as the magnetoresitance minima are due to the qualitative change of the magnetic scattering regime.

5. In order to combine results obtained by different methods, it is instructive to plot positions of the minima A, B, and C together with susceptibility data on the same B–T diagram (Fig. 4). The region of weak magnetic fields ($B < 0.1{-}0.15$ T) is characterized by a pronounced region of the intermediate phase and likely by a relatively small pocket for the spiral phase with long range magnetic order (Fig. 4) as follows from magnetic susceptibility data (Fig. 1). However, it should be noted that in contrast to the intermediate phase the existence of the spiral magnet phase at very low temperatures was so far not confirmed by direct magnetic structure studies even for $B = 0$. Therefore the part of the B–T diagram which corresponds to very low temperatures may be considered as hypothetical. Nevertheless, the magnetic susceptibility data (Fig. 1) may suggest that the transition temperature into spiral magnet phase should rapidly decrease with magnetic field as shown in Fig. 4. In principle, this type of magnetic phase diagram may indicate the presence of a field induced quantum critical point, but the study of this possibility is beyond the scope of this publication.

Let us now consider the region of high magnetic fields $B > 3.5$ T where the single minimum C of magnetoresistance exists. Previous studies have shown that this feature is typical for a transition between the paramagnetic and spin-polarized phases [10]. Therefore, in the considered range of magnetic fields the position of minimum C may mark the PM–SP phase boundary, i.e. the transition from thermally disordered spins into a state characterized by parallel alignment of spins. We emphasize that in the standard theory of ferromagnetism [16] the real phase transition between the paramagnetic and ferromagnetic phases does not exist for finite magnetic fields and from that point of view the experimental PM–SP phase boundary provided by minimum C may be a kind of crossover line. It is interesting, that in $Mn_{1-x}Fe_xSi$ this is not necessarily the case due to the expected formation of spin polarons in the vicinity of Mn magnetic moments just at PM–SP transition [10, 11, 14]. The latter assumption is strongly supported by magnetic resonance data [10, 11, 14] and

by the analysis of magnetic scattering [10]. In this case spin polarons may be considered as a quasi-bound states of itinerant electrons and manganese localized magnetic moments with an opposite orientation of Mn and electron spins. This ferrimagnetic-like spin ordering in the spin-polarized phase explains the observed reduction of the magnetic moment in the magnetically ordered phase of $Mn_{1-x}Fe_xSi$ as well as provides a way to natural interpretation of the recently discovered analogy in physical properties between MnSi and ferrimagnet Cu_2OSeO_3, which is a dielectric with Heisenberg localized magnetic moments [17]. Apparently, in the spin-polaron paradigm the standard limitation for ferromagnetic phase transition [16] is lifted and the PM–SP phase boundary may be sharp.

Considering the intermediate region of magnetic field $0.15\,\mathrm{T} < B < 3.5\,\mathrm{T}$, where two minima of magnetoresistance (A and B) exist, it is necessary to take into account the difference in magnitude of each peculiarity (Fig. 3). This difference is apparently related with the variation of magnetic structure at each possible phase transition. As long as the strongest difference in spin alignment is between the spin-polarized phase and the intermediate phase or the paramagnetic phase, it is possible to connect minimum A with the SP-phase – IP boundary (Fig. 4). Simultaneously the shallow minimum B (Fig. 3) may be attributed to the transition between the paramagnetic phase and the intermediate phase (note that the latter phase is characterized by a finite correlation length and by the absence of any long-range magnetic order as can be seen from Fig. 1). Additionally, the position of minimum B in the vicinity of T_s also supports this interpretation. This consideration provides the structure of the B–T magnetic phase diagram shown in Fig. 4. It is essential that for $0.1\,\mathrm{T} < B < 3.5\,\mathrm{T}$ the classically "forbidden" SP–PM phase boundary does not exist and the formation of the SP phase with lowering temperature is preceded by the transition into the intermediate phase.

Summarizing experimental results it is possible to deduce that in the studied sample for $B < 3.5\,\mathrm{T}$ the temperature lowering induces a phase transition from the PM to IP phase at $\sim$8–9 K. The increase of magnetic field first results in suppression of the transition into SM phase and then induces an onset of the transition into SP phase. The temperature of the IP–SP transition increases with magnetic field, so that at $B < 3.5\,\mathrm{T}$ the IP becomes suppressed (Fig. 4). It is worth noting that the intermediate phase with SRO is much more robust with respect to magnetic field than the spiral phase with LRO even in pure MnSi, where the application of a field of about $B \sim 0.6\,\mathrm{T}$ is sufficient to achieve the spin-polarized state [3]. Interesting, that in the studied range of magnetic fields the transition temperature into spin-polarized phase T_{SP} follows approximately the logarithmic law $T_{SP} \approx T_0 \log(B/B_0)$, where $T_0 \approx 2.7\,\mathrm{K}$ and $B_0 \approx 0.17\,\mathrm{T}$ (dashed line in Fig. 4). The latter parameter obtained from the fit of the $T_{SP}(B)$ experimental dependence in the range $0.5\,\mathrm{T} < B < 5\,\mathrm{T}$ is very close to the expected field where the transition into SM may be suppressed (Fig. 1).

6. Now it is possible to consider alternative interpretations of the IP region on the magnetic phase diagram. The observed temperature dependence of L_c for $T > 2\,\mathrm{K}$ allows to discuss the magnetic state of the intermediate phase as an extended region of magnetic fluctuations [2, 9] if one disregards the qualitative change of the diffraction pattern at T_s (Fig. 1) and corresponding analogy with liquid crystals [5–8]. It is important, that L_c tends to saturate at low temperatures indicating that the fluctuations becomes stabilized for $T < 2\,\mathrm{K}$. As long as spiral SRO in IP is conserved [2], it is possible to expect that the intermediate phase in $Mn_{1-x}Fe_xSi$ is a kind of chiral spin-liquid (SL) phase, which was predicted in the pioneering work [5]. However, the fact that the coherence length tends to saturate at $T \to 0$ may be related to the limited resolution function of the SANS setup. On the other hand, the shape of the diffraction peak is well described by the Lorentz function, which is reminiscent of fluctuating short-range correlations and therefore consistent with the interpretation of the intermediate phase as a SRO liquid-like phase. Apparently, the discussion of the SANS data solely can not provide completely decisive argument which allows eliminating fluctuations scenario, but in our opinion the obtained experimental data for $Mn_{1-x}Fe_xSi$ may be better explained in spin-liquid phase paradigm.

Another difficulty for the fluctuations model [9] arises from the magnetoresistance data (Figs. 2 and 3). When this ansatz is applied to the range $0.1\,\mathrm{T} < B < 3.5\,\mathrm{T}$ it is reasonable to assume that for $B = \mathrm{const}$ the formation of the phase where all spins are polarized with lowering temperature is preceded by gradual evolution of magnetic fluctuations in the paramagnetic phase (indeed a smooth variation of L_c is observed for $B = 0$, as it follows from Fig. 1). Therefore, a gradual evolution of magnetic scattering should be expected as well, and the appearance of the additional minimum B in the magnetoresistance temperature dependence, which manifests the change of the magnetic scattering regime, is very unlikely. Consequently the magnetoresistance data (Figs. 2 and 3) agree better with the concept where IP is treated as a real magnetic phase, which according to SANS data may be a SL phase.

In conclusion, following the analogy developed in [5], it is interesting to revisit considerations about paramagnetic, intermediate, and spin-polarized phases as magnetic replicas of gas, liquid, and solid phases, respectively. The SP phase with field induced long-range magnetic order is an analog of solid but apparently not a chiral solid (yet, it has been recently found by polarized neutron scattering that the spin excitations in the SP phase of pure MnSi are 100 % chiral objects [18]). At the same time the IP phase ("liquid") possesses short-range spiral magnetic order and, therefore, "melting" of the SP phase at finite magnetic field is accompanied by structural change, which is also the case of many real solids [19]. Our results suggest that the SP–IP "melting" curve meets the gas-liquid (PM–IP) boundary at a special point located at $T \sim 8.5$ K and $B \sim 3.5$ T. This point may be either a triple point if the spin-polaron scenario [10, 11] is valid for $Mn_{1-x}Fe_xSi$, or a critical point for the case of ferromagnet with weak Dzyaloshinskii–Moriya interaction. Therefore, further neutron scattering studies aimed at the investigation of the magnetic structure in the considered range of magnetic fields will be rewarding and will allow choosing between these two possibilities and shed more light on expected formation of the chiral spin-liquid phase in $Mn_{1-x}Fe_xSi$. Another interesting problem is the magnetic structure at very low temperatures, where a relatively weak magnetic field may induce a quantum phase transition, so that future research may enrich the received magnetic phase diagram of $Mn_{1-x}Fe_xSi$ system.

This work was supported by programmes of Russian Academy of Sciences "Electron spin resonance, spin-dependent electronic effects and spin technologies", "Electron correlations in strongly interacting systems" and by RFBR grant # 13-02-00160, and by projects VEGA 2/0106/13, APVV-14-0605, and by the CFNT MVEP project of the Slovak Academy of Sciences.

1. A. Bauer, A. Neubauer, C. Franz, W. Münzer, M. Garst, and C. Pfleiderer, Phys. Rev. B **82**, 064404 (2010).
2. S. V. Grigoriev, E. V. Moskvin, V. A. Dyadkin, D. Lamago, T. Wolf, H. Eckerlebe, and S. V. Maleyev, Phys. Rev. B **83**, 224411 (2011).
3. A. Bauer and C. Pfleiderer, Phys. Rev. B **85**, 214418 (2012).
4. S. V. Demishev, I. I. Lobanova, V. V. Glushkov, T. V. Ischenko, N. E. Sluchanko, V. A. Dyadkin, N. M. Potapova, and S. V. Grigoriev, JETP Lett. **98**, 829 (2013).
5. S. Tewari, D. Belitz, and T. R. Kirkpatrick, Phys. Rev. Lett. **96**, 047207 (2006).
6. F. Kruger, U. Karahasanovic, and A. G. Green, Phys. Rev. Lett. **108**, 067003 (2012).
7. A. Hamann, D. Lamago, Th. Wolf, H. v. Löhneysen, and D. Reznik, Phys. Rev. Lett. **107**, 037207 (2011).
8. L. M. Blinov, *Structure and Properties of Liquid Crystals*, Springer Dordrecht, Heidelberg, London, N.Y. (2011).
9. M. Janoschek, M. Garst, A. Bauer, P. Krautscheid, R. Georgii, P. Böni, and C. Pfleiderer, Phys. Rev. B **87**, 134407 (2013).
10. S. V. Demishev, V. V. Glushkov, I. I. Lobanova, M. A. Anisimov, V. Yu. Ivanov, T. V. Ishchenko, M. S. Karasev, N. A. Samarin, N. E. Sluchanko, V. M. Zimin, and A. V. Semeno, Phys. Rev. B **85**, 045131 (2012).
11. S. V. Demishev, A. N. Samarin, V. V. Glushkov, M. I. Gilmanov, I. I. Lobanova, N. A. Samarin, A. V. Semeno, N. E. Sluchanko, N. M. Chubova, V. A. Dyadkin, and S. V. Grigoriev, JETP Lett. **100**, 28 (2014).
12. T. Moriya, *Spin Fluctuations in Itinerant Electron Magnetism*, Springer-Verlag, Berlin, Heidelberg, N.Y., Tokyo (1985).
13. M. Corti, F. Carbone, M. Filibian, Th. Jarlborg, A. A. Nugroho, and P. Carretta, Phys. Rev. B **75**, 115111 (2007).
14. S. V. Demishev, A. V. Semeno, A. V. Bogach, V. V. Glushkov, N. E. Sluchanko, N. A. Samarin, and A. L. Chernobrovkin, JETP Lett. **93**, 213 (2011).
15. K. Yosida, Phys. Rev. **107**, 396 (1957).
16. S. V. Vonsovskii, *Magnetism*, John Wiley & Sons, N.Y. (1974).
17. V. A. Sidorov, A. E. Petrova, P. S. Berdonosov, V. A. Dolgikh, and S. M. Stishov, Phys. Rev. B **89**, 100403(R) (2014).
18. S. V. Grigoriev, A. S. Sukhanov, E. V. Altynbaev, S.-A. Siegfried, A. Heinemann, P. Kizhe, and S. V. Maleyev, Phys. Rev. B **92**, 220415(R) (2015).
19. S. M. Stishov, Sov. Phys. Usp. **11**, 816 (1969).